

## Abnormal thermal conductivity in tetragonal tungsten bronze $\text{Ba}_6 \times \text{Sr} \times \text{Nb}_{10}\text{O}_{30}$

T. Kolodiazny, H. Sakurai, O. Vasyukiv, H. Borodianska, and Y. Mozharivskyj

Citation: *Applied Physics Letters* **104**, 111903 (2014); doi: 10.1063/1.4868876

View online: <http://dx.doi.org/10.1063/1.4868876>

View Table of Contents: <http://scitation.aip.org/content/aip/journal/apl/104/11?ver=pdfcov>

Published by the AIP Publishing

### Articles you may be interested in

The crystal structure and magnetic properties of  $\text{Ba}_2\text{xSr}_\text{x}\text{Co}_2\text{Fe}_{12}\text{O}_{22}$

J. Appl. Phys. **115**, 17A523 (2014); 10.1063/1.4866892

Absence of tetragonal distortion in  $(1\text{x})\text{SrTiO}_3\text{-xBi}(\text{Zn}_{1/2}\text{Ti}_{1/2})\text{O}_3$  solid solution

J. Appl. Phys. **113**, 184109 (2013); 10.1063/1.4804934

Effects of Ca-substitution on structural, dielectric, and ferroelectric properties of  $\text{Ba}_5\text{SmTi}_3\text{Nb}_7\text{O}_{30}$  tungsten bronze ceramics

Appl. Phys. Lett. **101**, 042906 (2012); 10.1063/1.4739841

Giant dielectric response in  $(\text{Sm}_1 \times \text{Nd} \times)_{1.5}\text{Sr}_{0.5}\text{NiO}_4$  ceramics: The intrinsic and extrinsic effects

J. Appl. Phys. **112**, 024104 (2012); 10.1063/1.4737775

Relaxor ferroelectric characteristics of  $\text{Ba}_5\text{LaTi}_3\text{Nb}_7\text{O}_{30}$  tungsten bronze ceramics

Appl. Phys. Lett. **100**, 012902 (2012); 10.1063/1.3673913



**physicstoday**

Comment on any *Physics Today* article.

Measured energy in Japan  
David van Seggern  
(vsegger@seamless.com) University of Seattle  
July 2012, page 10  
DOI: 10.1063/1.3455555  
<http://dx.doi.org/10.1063/1.3455555>

The article by Thome Lar and Hideo Kanamori discusses the energy released by the 1994 Chubu earthquake. It is not right if the authors would have taken into account the energy released by the earthquake. They would find that the energy released by the earthquake is much larger than the energy released by the nuclear device. Therefore the parameters of the damage extend into the future when the released energy is that pushed upon, later becomes released in a new event. Perhaps calculations of one added that in, while another's calculations did not. E.M.C.

Written by Edgar Rucavitski, 14 July 2012 19:39

# Abnormal thermal conductivity in tetragonal tungsten bronze $\text{Ba}_{6-x}\text{Sr}_x\text{Nb}_{10}\text{O}_{30}$

T. Kolodiazhnyi,<sup>1(a)</sup> H. Sakurai,<sup>1</sup> O. Vasyukiv,<sup>1</sup> H. Borodianska,<sup>1</sup> and Y. Mozharivskyj<sup>2</sup>

<sup>1</sup>National Institute for Materials Science, Tsukuba, Ibaraki 305-0044, Japan

<sup>2</sup>Department of Chemistry and Chemical Biology, McMaster University, 1280 Main Street West, Hamilton, Ontario L8S4M1, Canada

(Received 5 March 2014; accepted 6 March 2014; published online 17 March 2014)

$\text{Ba}_{6-x}\text{Sr}_x\text{Nb}_{10}\text{O}_{30}$  solid solution with  $0 \leq x \leq 6$  crystallizes in centrosymmetric tetragonal “tungsten bronze” structure (space group  $P4/mbm$ ). We report on the  $x$  dependence of thermal conductivity of polycrystalline samples measured in the 2–400 K temperature interval. Substitution of Sr for Ba brings about a significant decrease in thermal conductivity at  $x \geq 3$  accompanied by development of a low-temperature ( $T \approx 10$ –30 K) “plateau” region reminiscent of a glass-like compounds. We explain this behaviour based on a size-driven site occupancy and atomic displacement parameters associated with an alkaline earth atomic positions in the title compounds. © 2014 AIP Publishing LLC.

[<http://dx.doi.org/10.1063/1.4868876>]

For decades thermal conductivity of amorphous solids has been a topic of fundamental interest in condensed matter physics.<sup>1–3</sup> With a resurgent activity in thermoelectrics, crystalline materials with high electrical conductivity and low (glassy-type) thermal conductivity are of special interest from both academic and industrial perspectives.

A common feature of potential thermoelectric materials is a presence of a low-energy fluctuations that can effectively scatter the heat-carrying acoustic phonons. These low-energy fluctuations include soft mode optical phonons,<sup>4</sup> magnons,<sup>5</sup> weakly bound “rattler” ions,<sup>6</sup> local elastic and electric dipoles,<sup>7</sup> etc.

Amorphous-type thermal conductivity,  $\kappa$ , is manifested by  $\kappa \propto T^2$  dependence for  $T \leq 1$  K and a  $\kappa$  plateau at  $T \approx 5$ –30 K. Thermal conductivity of several relaxor-type ferroelectric (FE) materials show amorphous-like features. These materials include disordered perovskites based on  $\text{PbMg}_{1/3}\text{Nb}_{2/3}\text{O}_3$ <sup>8</sup> and “dirty” displacive FE based on tetragonal tungsten bronze (TTB)  $\text{Ba}_{1-x}\text{Sr}_x\text{Nb}_2\text{O}_6$ .<sup>9,10</sup> In  $\text{PbMg}_{1/3}\text{Nb}_{2/3}\text{O}_3$ , the low-temperature  $\kappa$  plateau is ascribed to acoustic phonon interaction with a central mode associated with re-orientation and “breathing” of polar nano-regions.<sup>11</sup> The low- $T$   $\kappa$  dependence of the TTB-type  $\text{Ba}_{1-x}\text{Sr}_x\text{Nb}_2\text{O}_6$  is less understood as it has been studied for a very limited range of  $x$  (i.e.,  $x = 0.45$  and  $0.61$ ).<sup>10</sup> This is partially due to the fact that thermodynamically stable TTB structure of  $\text{Ba}_{1-x}\text{Sr}_x\text{Nb}_2\text{O}_6$  is formed only for  $0.25 \leq x \leq 0.75$ .<sup>12</sup>

The TTB structure of  $\text{Ba}_{1-x}\text{Sr}_x\text{Nb}_2\text{O}_6$  can be generally described as  $\text{A}_1\text{A}_2\text{A}_4\text{C}_4\text{B}_1\text{B}_2\text{O}_{30}$ . Tetragonal unit cell consists of a network of ten distorted corner sharing  $\text{NbO}_6$  octahedra which form square (A1-site), pentagonal (A2-site), and triangular (C-site) channels running along the  $c$ -axis. To maintain charge balance, five Ba and Sr ions are randomly distributed over six A1 and A2 sites, while one A-site per unit cell remaining vacant.<sup>12</sup> In view of these structural details, there might be several possible reasons for amorphous-like thermal conductivity in  $\text{Ba}_{1-x}\text{Sr}_x\text{Nb}_2\text{O}_6$ . These may include

random distribution of the A-site vacancies, Ba/Sr atomic disorder, soft-mode optical phonons associated with FE ground state.

In this contribution, we focus on the  $\text{Ba}_{6-x}\text{Sr}_x\text{Nb}_{10}\text{O}_{30}$  compound which is structurally isomorphous with the TTB-type  $\text{Ba}_{1-x}\text{Sr}_x\text{Nb}_2\text{O}_6$ . In contrast to  $\text{Ba}_{1-x}\text{Sr}_x\text{Nb}_2\text{O}_6$ , the  $\text{Ba}_{6-x}\text{Sr}_x\text{Nb}_{10}\text{O}_{30}$  compound does not contain the A-site vacancies because they are filled with Sr/Ba ions. Furthermore, it forms complete solid solution with  $0 \leq x \leq 6$ .<sup>13–15</sup> This offers a unique opportunity to explore the effect of the A-site ionic size on the thermal conductivity of  $\text{Ba}_{6-x}\text{Sr}_x\text{Nb}_{10}\text{O}_{30}$  in an absence of the A-site vacancies.

Polycrystalline samples were prepared from 99.99% pure  $\text{BaCO}_3$  and  $\text{SrCO}_3$  (Wako Chemicals, Japan) and 99.998%  $\text{Nb}_2\text{O}_5$  (Cerac, USA). The stoichiometric mixtures were treated at 1000 °C for 10 h in flowing 3%  $\text{H}_2/\text{Ar}$  gas with 2 intermediate re-grindings. Dense ceramic bodies were sintered in flowing 3%  $\text{H}_2/\text{Ar}$  gas at 1360 °C for 10 h. Phase composition was studied by powder X-ray diffraction (Rigaku Ultima III X-ray diffractometer with  $\text{Cu } K_\alpha$  X-ray source). Lattice parameters, site occupancies, and isotropic atomic displacement parameters (ADPs) were obtained from Rietveld refinement of the X-ray data using Jana2006.<sup>16</sup> For thermal conductivity measurements, samples were cut into rectangular bars of  $1.8 \times 1.8 \times 12$  mm. Four gold-plated copper leads were attached to the samples with silver epoxy. Physical property measurements system (PPMS, Quantum Design, USA) was used for  $\kappa$  measurements in a temperature interval of 2–400 K.

Figure 1 shows temperature dependence of  $\kappa$  for  $\text{Ba}_{6-x}\text{Sr}_x\text{Nb}_{10}\text{O}_{30}$  with  $0 \leq x \leq 6$ . High- $T$   $\kappa$  values range from 1 to 4  $\text{W K}^{-1} \text{m}^{-1}$  for  $x = 6$  and 0, respectively. These  $\kappa$  values for the A-site filled  $\text{Ba}_{6-x}\text{Sr}_x\text{Nb}_{10}\text{O}_{30}$  are in a ballpark of the thermal conductivities reported for the A-site deficient TTB-type  $\text{Ba}_{1-x}\text{Sr}_x\text{Nb}_2\text{O}_6$  compounds.<sup>17</sup> We conclude, therefore, that the A-site vacancy does not play a crucial role in defining the low  $\kappa$  in the TTB compounds. According to Fig. 1, substitution of Sr for Ba results in the overall decrease in  $\kappa$ . At low temperature,  $\kappa$  develops a

<sup>a)</sup>Electronic mail: kolodiazhnyi.taras@nims.go.jp

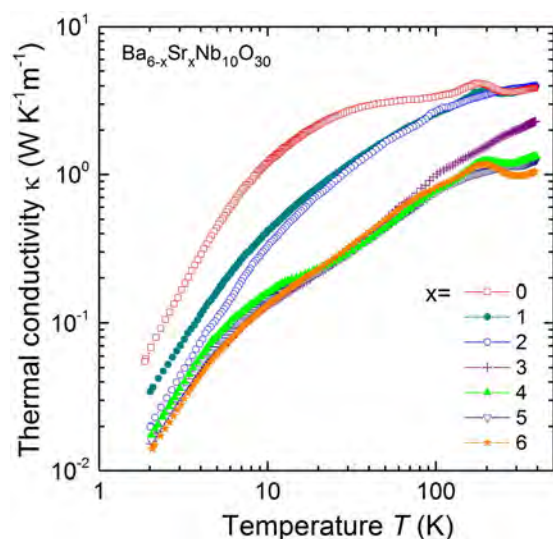


FIG. 1. Thermal conductivity of  $\text{Ba}_{6-x}\text{Sr}_x\text{Nb}_{10}\text{O}_{30}$ . The experimental error in the  $\kappa$  value is  $\pm 0.1$  and  $\pm 0.001 \text{ W K}^{-1} \text{ m}^{-1}$  at 400 and 2 K, respectively.

“plateau”-like anomaly at  $10 \leq T \leq 30 \text{ K}$  resembling the one observed in amorphous solids and  $\text{PbMg}_{1/3}\text{Nb}_{2/3}\text{O}_3$ -based relaxor FE.<sup>11</sup> At higher temperatures ( $T > 100 \text{ K}$ ), most of the samples show a broad peak followed by a further gradual increase in  $\kappa$  (Fig. 1). Qualitatively similar peak at 380 K associated with a structural transition from high- $T$  paraelectric to low- $T$  FE phase was reported for  $\text{Ba}_{0.48}\text{Sr}_{0.52}\text{Nb}_2\text{O}_6$  in Ref. 17.

The temperature and  $x$ -dependence of  $\kappa$  of the title compounds is unusual from several perspectives. First, according to Berman, the simplest expression for thermal conductivity of non-metallic crystal is given by<sup>18</sup>

$$\kappa = \frac{1}{3} C v l, \quad (1)$$

where  $C$  is the heat capacity per unit volume contributed by phonons,  $v$  is the mean phonon velocity, and  $l$  is the mean free path of the acoustic phonons. Because  $v \propto M^{-1/2}$  (where  $M$  is effective mass of the phonon mode), the Ba-rich  $\text{Ba}_{6-x}\text{Sr}_x\text{Nb}_{10}\text{O}_{30}$  compounds should demonstrate lower thermal conductivity than their Sr-rich counterparts. This is exactly opposite to the experimental data in Fig. 1. Second, a random occupation of the A-sites by Sr/Ba atoms at intermediate  $x$  values is expected to cause a so-called “mass defect” phonon scattering when phonon impacts the atomic defect with a different mass.<sup>19</sup> This type of phonon scattering is expected to bring about a global  $\kappa(x)$  minimum at  $x \approx 3$ . Contrary to this rationale, no such a minimum is detected in the  $\kappa(x)$  dependence shown in Fig. 2. Finally, it is not clear why a “plateau”-like  $\kappa(T)$  anomaly is found only at  $x > 3$  given a structurally isomorphous nature of the  $\text{Ba}_6\text{Nb}_{10}\text{O}_{30}$  and  $\text{Sr}_6\text{Nb}_{10}\text{O}_{30}$  end members.

For an answer to these questions, we look for small differences in the structural atomic parameters of the title compounds. Room-temperature Rietveld refinement of the X-ray diffraction patterns (Fig. 3) confirms that the  $\text{Ba}_{6-x}\text{Sr}_x\text{Nb}_{10}\text{O}_{30}$  series crystallizes in centro-symmetric  $P4/mbm$  space group.<sup>15</sup> The  $a$  lattice parameter, however, shows a clear positive deviation from the ideal solid solution

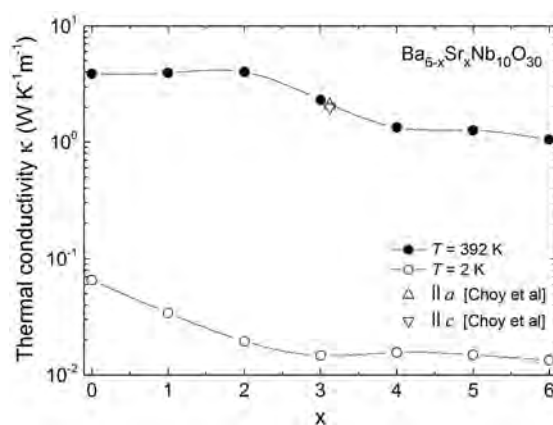


FIG. 2. Concentration dependence of thermal conductivity of polycrystalline  $\text{Ba}_{6-x}\text{Sr}_x\text{Nb}_{10}\text{O}_{30}$  measured at 2 and 392 K. Partially overlapping “up” and “down” triangles show single crystal data for  $\text{Ba}_{0.48}\text{Sr}_{0.52}\text{Nb}_2\text{O}_6$  measured along the  $a$  and  $c$ -axis at 395 K adapted from Ref. 17. The lines are the guides for the eye.

behavior (Fig. 4(a)), which is an indication that the Ba/Sr ions show a preferential occupancy of the A1/A2 sites. Indeed, Reitveld refinement of the atomic occupancy of the A1/A2 sites reveals that the cubo-octahedral A1 sites are preferentially occupied by smaller  $\text{Sr}^{2+}$  ions, whereas large voids of the tricapped trigonal prismatic A2 sites are favored by the larger  $\text{Ba}^{2+}$  ions.

Once the Sr concentration exceeds  $x \approx 2$ , the  $\text{Sr}^{2+}$  ions start occupying the large A2 sites. This trend is also reflected by an increase in the isotropic ADP,  $U_{iso}$ , of the A2-site for  $x > 2$ . The isotropic ADPs of the A1, A2, Nb1, and Nb2 lattice sites are plotted in Figure 4(b).

The ADPs for cubo-octahedral A1 site are non-exceptional. Within one standard deviation they are comparable with  $U_{eq} = 0.0139$  and  $0.00794 \text{ \AA}^2$  for  $\text{Sr}^{2+}$  and  $\text{Ba}^{2+}$  in perovskite-type  $\text{Sr}_{0.92}\text{NbO}_3$  and  $\text{Ba}_{0.95}\text{NbO}_3$ , respectively.<sup>20,21</sup> On the other hand, the large ADPs (e.g.,  $U_{iso} > 0.02 \text{ \AA}^2$ ) for A2 site in the  $\text{Ba}_{6-x}\text{Sr}_x\text{Nb}_{10}\text{O}_{30}$  are definitely abnormal. They indicate that  $\text{Ba}^{2+}$ , and especially  $\text{Sr}^{2+}$  ion, in the A2 site is loosely bound to the oxygen

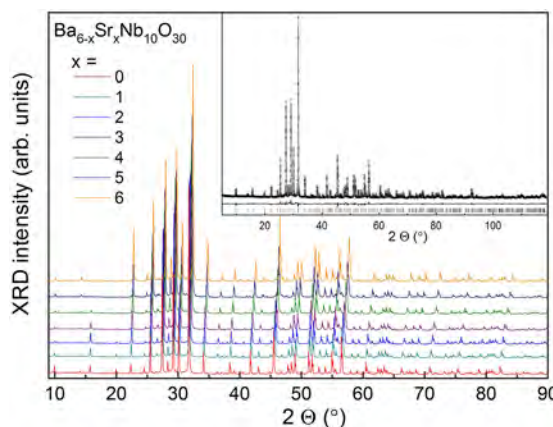


FIG. 3. Room-temperature X-ray diffraction profiles for  $\text{Ba}_{6-x}\text{Sr}_x\text{Nb}_{10}\text{O}_{30}$ . In the inset, the experimental X-ray diffraction pattern of  $\text{Ba}_6\text{Nb}_{10}\text{O}_{30}$  is shown by open circles. Calculated diffraction pattern from Rietveld refinement and the difference between observed and calculated data are shown by solid lines. The vertical bars at the bottom of the plot indicate the positions of expected Bragg peaks.



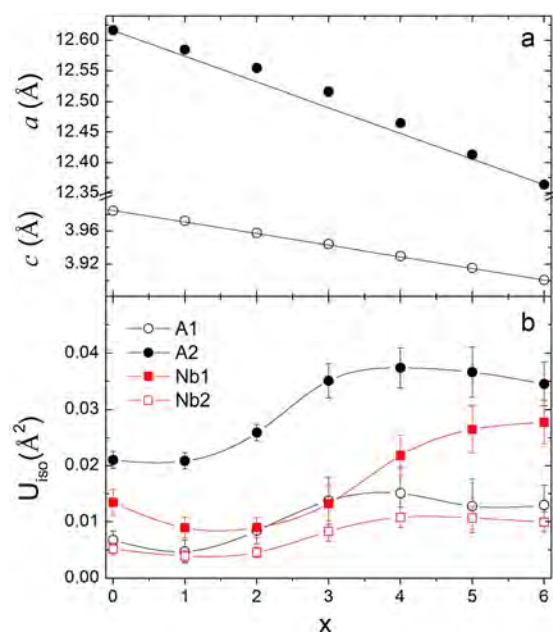


FIG. 4. (a) Evolution of the lattice constants  $a$  and  $c$  as a function of Sr content,  $x$ , in  $\text{Ba}_{6-x}\text{Sr}_x\text{Nb}_{10}\text{O}_{30}$ . Please note a positive deviation from the Vegard's law for  $a$ . (b) Isotropic displacement parameters,  $U_{iso}$ , for A1, A2, Nb1, and Nb2 lattice sites as a function of  $x$ . Vertical bars represent one standard deviation. The lines are the guides for the eye.

ligands. The ions either undergo a large dynamic displacements in a single U-shape potential well or they may have a static off-center multi-well ground state. The room temperature ADP data alone, however, cannot distinguish between the static and dynamic disorder of the A2 atoms in the title compounds.

One may notice a close correlation between the thermal conductivity data in Fig. 2 and the ADP data in Fig. 4(b). High- $T$   $\kappa$  shows a pronounced decrease at  $x > 2$  which is mirrored by an increase in the A2  $U_{iso}$ . A weakly bound Sr in an oversized atomic cage undergoing a large localized vibrations may be referred to as a “rattler.” If its Einstein frequency is low enough, it can effectively scatter heat-carrying acoustic phonons and also result in the low- $T$   $\kappa$  plateau.<sup>6</sup> Alternative to this mechanism, Sr ions in the A2 sites may undergo static off-center displacements. If these displacements are random, a large density of symmetry-breaking defects will be created. Phonon-assisted tunneling between random off-center Sr positions may also be responsible for the low- $T$  “plateau”-like  $\kappa$  anomaly. This picture appears to be very similar to that reported for Ba-, Sr-, and Eu-doped germanium clathrates.<sup>22</sup>

While there is a clear correlation between the ADP and the thermal conductivity, there are still a number of open questions. It remains to be clarified whether the title

compounds undergo a low-temperature transition to the FE phase and, if they do, what is the effect, if any, of the FE phase on the thermal conductivity of  $\text{Ba}_{6-x}\text{Sr}_x\text{Nb}_{10}\text{O}_{30}$ . In a wake of a recent criticism of the “rattler” model,<sup>23</sup> it is important to understand whether the  $\text{Ba}^{2+}$  and  $\text{Sr}^{2+}$  ions in the A2 site are truly decoupled from the host oxygen ligands. Finally, it is interesting to see what is the effect of the abnormal thermal conductivity on the electron transport in the title compounds. These topics will be addressed in the forthcoming publications.

This work was supported by Grant-in-Aid for Scientific Research C 21560025 from JSPS provided to T.K.

- <sup>1</sup>R. C. Zeller and R. O. Pohl, *Phys. Rev. B* **4**, 2029 (1971).
- <sup>2</sup>E. R. Grannan, M. Randeria, and J. P. Sethna, *Phys. Rev. Lett.* **60**, 1402 (1988).
- <sup>3</sup>L. Gil, M. A. Ramos, A. Bringer, and U. Buchenau, *Phys. Rev. Lett.* **70**, 182 (1993).
- <sup>4</sup>O. Delaire, J. Ma, K. Marty, A. F. May, M. A. McGuire, M.-H. Du, D. J. Singh, A. Podlesnyak, G. Ehlers, M. D. Lumsden, and B. C. Sales, *Nature Mater.* **10**, 614 (2011).
- <sup>5</sup>O. Delaire, M. B. Stone, J. Ma, A. Huq, D. Gout, C. Brown, K. F. Wang, and Z. F. Ren, *Phys. Rev. B* **85**, 064405 (2012).
- <sup>6</sup>V. Keppens, D. Mandrus, B. C. Sales, B. C. Chakoumakos, P. Dai, R. Coldea, M. B. Maple, D. A. Gajewski, E. J. Freeman, and S. Bennington, *Nature* **395**, 876 (1998).
- <sup>7</sup>F. Cordero, M. Corti, F. Craciun, C. Galassi, D. Piazza, and F. Tabak, *Phys. Rev. B* **71**, 094112 (2005).
- <sup>8</sup>D. A. Ackerman, D. Moy, R. C. Potter, A. C. Anderson, and W. N. Lawless, *Phys. Rev. B* **23**, 3886 (1981).
- <sup>9</sup>G. Burns, *Phys. Rev. B* **13**, 215 (1976).
- <sup>10</sup>E. Fischer, W. Hässler, and E. Hegenbarth, *Phys. Status Solidi A* **72**, K169 (1982).
- <sup>11</sup>M. Tachibana and E. Takayama-Muromachi, *Phys. Rev. B* **79**, 100104(R) (2009); and references therein.
- <sup>12</sup>P. B. Jamieson, S. C. Abrahams, and J. L. Bernstein, *J. Chem. Phys.* **48**, 5048 (1968).
- <sup>13</sup>A. Von Feltz and H. Langbein, *Z. Anorg. Allg. Chem.* **47**, 425 (1976).
- <sup>14</sup>N. Nguyen, J. Choisnet, and B. Raveau, *C. R. Acad. Sci. Paris C* **282**, 303 (1976).
- <sup>15</sup>B. Hessen, S. A. Sunshine, A. T. Siegrist, A. T. Fiory, and J. V. Wazczak, *Chem. Mater.* **3**, 528 (1991).
- <sup>16</sup>V. Petricek, M. Dusek, and L. Palatinus, Jana2006: The Crystallographic Computing System, Institute of Physics, Praha, Czech Republic. URL: <http://jana.fzu.cz/>.
- <sup>17</sup>C. L. Choy, W. P. Leung, T. G. Xi, Y. Fei, and C. F. Shao, *J. Appl. Phys.* **71**, 170 (1992).
- <sup>18</sup>R. Berman, *Thermal Conduction in Solids* (Clarendon, Oxford, 1976).
- <sup>19</sup>J. Callaway and H. C. von Baeyer, *Phys. Rev.* **120**, 1149 (1960).
- <sup>20</sup>R. B. Macquart, B. J. Kennedy, and M. Avdeev, *J. Solid State Chem.* **183**, 2400 (2010).
- <sup>21</sup>B. Hessen, S. A. Sunshine, T. Siegrist, and R. Jimenez, *Mater. Res. Bull.* **26**, 85 (1991).
- <sup>22</sup>B. S. Sales, B. C. Chakoumakos, R. Jin, J. R. Thompson, and D. Mandrus, *Phys. Rev. B* **63**, 245113 (2001).
- <sup>23</sup>M. M. Koza, M. R. Johnson, R. Vienneis, H. Mutka, L. Girard, and D. Ravot, *Nature Mater.* **7**, 805 (2008).